Effects of paramagnons in a proximity sandwich

H. G. Zarate and J. P. Carbotte
Department of Physics, McMaster University, Hamilton, Ontario, Canada L8S 4M1
(Received 12 August 1985; revised manuscript received 2 June 1986)

We have studied the effects that the existence of spin fluctuations on the normal side of a proximity sandwich can have on superconducting properties. We consider the critical temperature, its functional derivative with paramagnon spectral density, the frequency-dependent gap, and the quasiparticle density of states. The question of the interplay of phonon and paramagnon structure in tunneling characteristics is addressed. Comparison with experiment is made for the case of Pd.

I. INTRODUCTION

It has long been thought that Pd is not observed to be a superconductor[1] down to the lowest temperatures tested [~ 2 mK (Ref. 2)] because of the inhibiting effects of "spin fluctuations" or "paramagnons" which are pair breaking. The possible existence of spin fluctuations is linked to its strongly enhanced spin susceptibility[3] and attendant large temperature dependence.[4] The Stoner enhancement factor of Pd is 9.3,[4] and the characteristic spin-fluctuation temperature (T_{SF}) has been estimated to be as low as 250 K.[3,5,6]

A metal which may have even larger spin-fluctuation effects is $TiBe_2$. Its Stoner factor is 65 (Ref. 4) with a very strong temperature dependence in the susceptibility.[7,8] Also, the low-temperature electronic specific heat (C) is clearly observed to bend upward at low temperature on a C/T versus T^2 plot (T is the temperature). This indicates fairly unambiguously[9,10] a $(T/T_{SF})^2\ln(T/T_{SF})$ term as predicted in theories of paramagnons.[11,12] Even more importantly, in building a case that spin fluctuations exist in this material, is the fact that the $(T/T_{SF})^2\ln(T/T_{SF})$ is largely quenched by an external magnetic field of 17 T (Ref. 10) in accord with theoretical expectations.[13] The characteristic spin-fluctuation temperature $T_{SF}=2.5$ meV is very low and a rough estimate of the electron mass enhancement factor due to paramagnons is $\lambda_{SF}\cong 0.5$.[9,10] In such a system there should be large effects introduced by the paramagnons when superconductivity is induced in it by placing it in proximity to a good superconductor such as Pb.

In intrinsic superconductors the possibility of paramagnon effects has been extensively studied[14–21] in recent years, but no definitive conclusion has yet been reached, possibly because the values of λ_{SF} are small and the characteristic temperature T_{SF} large. If T_{SF} is much larger than a phonon energy, paramagnons simply lead to a constant renormalization[17–20] of the electron-phonon interaction so that there is no easily identifiable trace of their existence. This should not be the case for systems with small T_{SF} for which the paramagnon spectral density should be directly reflected in the current voltage (I-V) characteristic of a tunnel junction at low energies.

In this paper we study the effect of low-energy paramagnons on the superconducting properties of a proximity sandwich. The normal and superconducting side are coupled to each other according to the McMillan[22] tunneling model. This should be adequate for our work since one of our main purposes is to study the structure in I-V characteristics that results from the phonons and paramagnons on the normal side. While the induced Pb phonon structure may not always be well represented by the model and interference effects due to reflections at film boundaries are left out, the McMillan model was found to be quite adequate in our previous consideration of phonon structure in Cu sandwiches.[23] While it is true that boundary scattering[24–26] could affect the paramagnon spectral density [$P(\omega)$], particularly at low energies, here we take the approach that $P(\omega)$ is to be determined from tunneling experiments and so contains all these complications. Thus no attempt is made to calculate it directly from first principles. In fact, paramagnon theory remains at such a primitive level[27] that it could not be expected to yield qualitatively reliable results.

In Sec. II the necessary set of four linearized Eliashberg equations written on the imaginary frequency axis[24–27] are given and solved numerically. They are needed to study the effect on the junction critical temperature T_c^{NS} of the existence of a paramagnon spectral density $P_N(\omega)$ on the normal side. Numerical solutions for T_c^{NS} are presented for $P_N(\omega)\neq 0$ and compared with the $P_N(\omega)=0$ case. In addition, the functional derivative of T_c^{NS}, with respect to $P_N(\omega)$, is derived in a simple approximation for the case of no net interaction on the normal side (the main derivation is contained in an appendix.) It is found that paramagnons are increasingly more effective in reducing T_c^{NS} as their energy is lowered. In Sec. III we introduce the real frequency axis version of the Eliashberg equation at zero temperature ($T=0$).[23] Solutions of the equations for the real and imaginary part of the gap on normal and superconducting sides are given and paramagnon structures discussed. From these solutions, the I-V characteristics of the normal side are computed and the characteristic signature of the paramagnons in d^2V/dI^2 described. Also, an extensive discussion is given of the interplay of phonon and paramagnon structure when T_{SF} is

comparable in size to the Debye temperature. In Sec. IV the specific case of Pd is considered in some detail while in a last section (V) we draw some conclusions.

II. PARAMAGNONS ON SANDWICH CRITICAL TEMPERATURE

For the critical temperature (T_c^{NS}) the linearized Eliashberg equations hold. On the imaginary frequency axis with $\omega_n \equiv \pi T_c(2n-1)$ they are[21-23]

$$\tilde{\Delta}_S(n)=\pi T_c \sum_m [\lambda_S^-(m-n)-\mu_S^*] \times \frac{\tilde{\Delta}_S(m)}{|\tilde{\omega}_S(m)|}+\Gamma_S \frac{\tilde{\Delta}_N(n)}{|\tilde{\omega}_N(n)|} , \quad (1)$$

$$\tilde{\omega}_S(n)=\omega_n+\pi T_c \sum_m \lambda_S^+(m-n)\mathrm{sgn}\omega_m+\Gamma_S \mathrm{sgn}\omega_n \quad (2)$$

and

$$\tilde{\Delta}_N(n)=\pi T_c \sum_m [\lambda_N^-(m-n)-\mu_N^*] \times \frac{\tilde{\Delta}_N(m)}{|\tilde{\omega}_N(m)|}+\Gamma_N \frac{\tilde{\Delta}_S(n)}{|\tilde{\omega}_S(n)|} , \quad (1')$$

$$\tilde{\omega}_N(n)=\omega_n+\pi T_c \sum_m \lambda_N^+(m-n)\mathrm{sgn}\omega_m+\Gamma_N \mathrm{sgn}\omega_n . \quad (2')$$

In these equations $\tilde{\Delta}_{S,N}(n)$ are the pairing energy on the superconducting and normal side of the sandwich, respectively, with $\tilde{\omega}_{S,N}$ the renormalization $Z(i\omega_n)$ times ω_n. The coupling between the two sides enter through the McMillan tunneling parameters Γ_N, Γ_S, one of which is taken to be an adjustable parameter with

$$\frac{\Gamma_S}{\Gamma_N}=\frac{d_N N_N(0)}{d_S N_S(0)} . \quad (3)$$

In Eq. (3), d_N and d_S are the normal and superconducting layer thicknesses and $N_N(0)$ ($N_S(0)$) the electronic density of state on the normal (superconducting) side. The Coulomb pseudopotential is denoted by $\mu_{N,S}^*$ and $\lambda_{N,S}^{\pm}(m-n)$ is related to the spectral densities on each side,

$$\lambda_{N,S}^{\pm}(m-n)=\int \frac{2\Omega[\alpha_{N,S}^2 F(\Omega)\pm P_{N,S}(\Omega)]}{\Omega^2+(\omega_n-\omega_m)^2} d\Omega \quad (4)$$

with $\alpha^2 F(\Omega)$ [$P(\Omega)$] the electron-phonon (paramagnon) spectral density. For the superconducting side we take $\alpha_S^2 F(\Omega)$ to be that of Pb (Ref. 28) and $P_S(\Omega)\equiv 0$.

To illustrate the effect that the presence of paramagnons on the normal side of a proximity sandwich introduce on its critical temperature, we consider two systems. We study Pb in proximity with a normal material that has $P_N(\Omega)$ given by a Lorentzian distribution peaked at 2.5 meV with a width of 2 meV and a paramagnon mass renormalization constant

$$\left[\lambda_{SF}=2\int \frac{P_N(\omega)d\omega}{\omega}\right]_{\lambda_{SF}=0.7}$$

(system I). We do not include any attraction produced by phonons, but include a Coulomb repulsion of $\mu_N^*=0.1$. We compare this system with the case in which the normal material has no phonons and also no paramagnons and the same value of μ_N^* (system II).

Figure I gives the critical temperature T_c^{NS} of the sandwich, Pb-normal metal, normalized to the Pb value (T_c^{Pb}) as a function of the coupling parameter Γ_S for two different values of Γ_N. The solid line corresponds to Γ_N very small, $\Gamma_N \lesssim 0.1$ meV with $\lambda_{SF}=0$ (system II), while the points denoted by plus signs (+) indicate the results obtained for system I with the same value of Γ_N. We see that in this limit the two systems give almost the same variation of T_c^{NS}/T_c^{Pb} versus Γ_S and that this variation follows very closely the Abrikosov-Gorkov results. Note that the results for system I (with paramagnons) end at $T_c^{NS}/T_c^{Pb}\cong 0.45$. Below this value of the reduced temperature, we were no longer able to converge our results.

The dashed line in Fig. 1 is for system I but with $\Gamma_N=1.0$ meV (a smaller thickness of normal metal relative to the superconducting thickness than previously considered). It is seen that this curve lies far below the one for the system with no paramagnons (system II) with the same value of Γ_N which is represented by the dotted line. The differences between the two curves increase markedly with increasing Γ_S. It is important to note, however, that such a comparison may not be quite fair when it is realized that Γ_N is a fitting parameter when a comparison of theory with experiment is attempted. In this regard we need to keep in mind that in reducing Eqs. (1) and (2) in a Bardeen-Cooper-Schrieffer (BCS-) type model, Γ_S and Γ_N get renormalized by $1+\lambda_S^+(0)$ and $1+\lambda_N^+(0)$, respective-

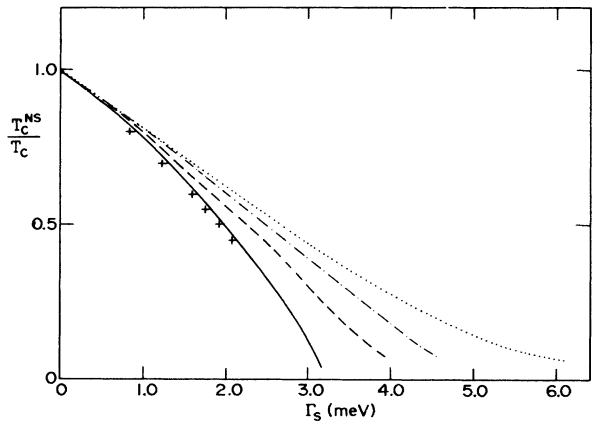

FIG. 1. Critical temperature T_c^{NS} of a proximity sandwich with Pb on the superconducting side and a material in which paramagnons are present on the normal side. The T_c^{NS} values are normalized to the T_c of Pb (T_c^{Pb}). The solid line is for $\Gamma_N=0.1$ meV and $\lambda_{SF}=0$ and is close to the Abrikosov-Gorkov variation. The points denoted by plus signs (+) are for the same Γ_N but with $\lambda_{SF}=0.7$. The dashed line is for $\Gamma_N=1$ meV and $\lambda_{SF}=0.7$, the dashed-dotted line for $\Gamma_N=1.7$ meV and $\lambda_{SF}=0.7$, and the dotted line is for $\Gamma_N=1$ meV and $\lambda_{SF}=0$. In all cases $\mu_N^*=0.1$.

ly. This is discussed by Mitrović.[6]

If $\lambda^{\pm}(n-m)$ is approximated by a constant value $\lambda^{\pm}(0)\equiv\lambda^{\pm}$ for $|\omega_n|$ and $|\omega_m|$ less than some cutoff ω_c and zero otherwise, we get for (1) and (2)

$$\Delta_{S,N}(n)=\left[\frac{\lambda^{-}_{S,N}-\mu^{*}_{S,N}}{\lambda^{+}_{S,N}+1}\right]\pi T_c \times \sum_{\substack{m,\\ |\omega_m|<\omega_c}} \frac{\Delta_{S,N}(m)}{|\omega^{0}_{S,N}(m)|}+\overline{\Gamma}_{S,N}\frac{\Delta_{N,S}(n)}{|\omega^{0}_{N,S}(n)|} \tag{5a}$$

and

$$\omega^{0}_{S,N}(n)=\omega_n+\overline{\Gamma}_{S,N}\,\mathrm{sgn}\omega_n \tag{5b}$$

with

$$\tilde{\Delta}_{N,S}(n)=(1+\lambda^{+}_{S,N})\Delta_{S,N} \tag{6a}$$

and

$$\overline{\Gamma}_{S,N}=\frac{\Gamma_{S,N}}{(1+\lambda^{+}_{S,N})}\ . \tag{6b}$$

The above would indicate that when comparing results for systems I and II we should perhaps recognize from the outset that one effect of paramagnons on the normal side is to renormalize Γ_N by a factor of $(1+\lambda_{SF})^{-1}$. The dashed-dotted curve in Fig. 1 is for system I with $\Gamma_N=1.7$ meV which corresponds to a renormalized $\overline{\Gamma}_N=1$. It is seen that even when Γ_N is increased to 1.7 meV the curve for T_c^{NS}/T_c^{Pb} is still significantly below the dotted curve which applies to system II. Thus, even when a renormalization of Γ_N is accounted for, the curves for the variation of the normalized junction temperature against Γ_S do not follow the same pattern with and without paramagnons. Difference certainly arise which reflect the presence of paramagnons in the normal side of the junction which go beyond a renormalization of Γ_N.

In a later section, after we have presented the real axis version of the Eliashberg equations, we will discuss, in parallel fashion to what we have just done for the critical temperature, the effect of $P_N(\omega)$ on the normal side gap edge Ω_N. It will be found to be reduced by $P_N(\omega)$ in a similar fashion to the junction critical temperature T_c^{NS}.

It is interesting to know how the position in energy of the spin fluctuations affects the junction critical temperature. Such a question can be answered directly from functional derivative considerations. In the Appendix we give a derivation of a simple formula for the functional derivative of T_c^{NS} with $P_N(\omega)$ of the normal side. $\delta T_c^{NS}/\delta P_N(\Omega_0)$ gives the effectiveness in depressing the junction temperature of adding an infinitesimal amount of paramagnon spectral weight, at frequency Ω_0. In Fig. 2 we compare results for $\delta T_c^{NS}/\delta P_N(\Omega_0)$ with similar results for $\delta T_c^{NS}/\delta\alpha_N^2F(\Omega_0)$ which can be obtained from formula (A14) on changing the sign in front of the first of the two sums. We see that paramagnons always reduce T_c and become increasingly more effective as the frequency Ω_0 tends to zero. In fact, the functional derivative diverges like $1/\Omega_0$ as $\Omega_0\to 0$. This divergence comes from the $n=m$ term in the double sum of (A14). By contrast, this term cancels out for $\delta T_c^{NS}/\delta\alpha_N^2F(\Omega_0)$, and in this case the functional derivative goes to zero at $\Omega_0\to 0$ having had a maximum at a higher frequency around $7k_BT_c^0$. Note that what is plotted in Fig. 2 is $\delta T_c'/\delta P_N(\Omega_0)$ and $\delta T_c'/\delta\alpha_N^2F(\omega)$, which differ from the actual functional derivatives by the numerical factor

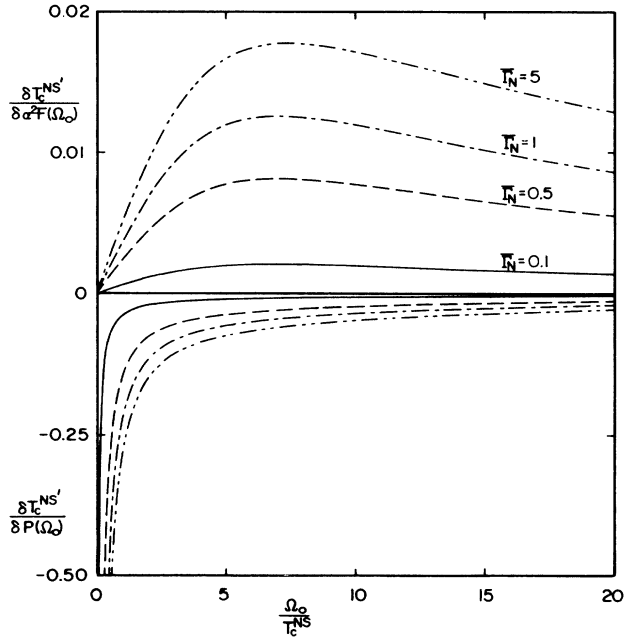

FIG. 2. Functional derivatives of the critical temperature of a proximity sandwich. The top curve gives functional derivative with respect to the electron-phonon spectral density $\delta T_c^{NS}/\delta\alpha_N^2F(\Omega_0)$ and the bottom curve the functional derivative with respect to the paramagnon spectral density $\delta T_c^{NS}/\delta P_N(\Omega_0)$. In each curve the proportionality factor

$$\frac{\overline{\Gamma}_N\overline{\Gamma}_S}{\pi(1+\lambda_N^{+})}\frac{1}{1-\dfrac{\overline{\Gamma}_S}{2\pi k_BT_c^0}\psi'\left[\dfrac{\overline{\Gamma}}{2\pi k_BT_c^0}+\dfrac{1}{2}\right]}$$

has been left out and only the remaining sums in Eq. (A14) are included.

$$\frac{\overline{\Gamma}_N\overline{\Gamma}_S}{\pi(1+\lambda_N^{+})}\frac{1}{1-(\overline{\Gamma}_S/2\pi k_BT_c^0)\psi'(\overline{\Gamma}/2\pi k_BT_c^0+\frac{1}{2})}\ . \tag{7}$$

This was done for clarity since it does not change the shape of the curve. It should be remembered, however, that the absolute value of $\delta T_c^{NS}/\delta P_n(\omega)$ is additionally proportional to each $\overline{\Gamma}_N$ and $\overline{\Gamma}_S$. This makes sense since for small $\overline{\Gamma}_S$ there is only a very small layer of normal metal compared to superconductor and so the normal side

can have little effect on the junction temperature. For $\bar{\Gamma}_N$ small the opposite holds and the junction temperature itself is small. We next consider the gap at zero temperature.

III. GAP AND I-V CHARACTERISTICS

To calculate the current-voltage (I-V) characteristics expected from a proximity sandwich with paramagnons on the normal side it is most convenient to use the zero-temperature Eliashberg equations written on the real axis.[23] The necessary equations are[22,23,28]

$$\Delta_{N,S}(\omega)Z_{N,S}(\omega)=\phi^P_{N,S}(\omega)+\frac{i\Gamma_{N,S}\Delta_{S,N}(\omega)}{[\omega^2-\Delta^2_{S,N}(\omega)]^{1/2}}\ , \tag{8}$$

$$Z_{N,S}(\omega)=Z^P_{N,S}(\omega)+\frac{i\Gamma_{N,S}}{[\omega^2-\Delta^2_{S,N}(\omega)]^{1/2}} \tag{9}$$

with

$$\phi^P_{N,S}(\omega)=\int_0^{\omega_c}d\omega'\,\mathrm{Re}\left[\frac{\Delta_{N,S}(\omega')}{[(\omega')^2-\Delta^2_{N,S}(\omega')]^{1/2}}\right]\left[\int d\nu[\alpha^2_{N,S}F(\nu)-P_{N,S}(\nu)]\left[\frac{1}{\omega'+\omega+\nu-i0^+}+\frac{1}{\omega'-\omega+\nu-i0^+}\right]-\mu^*\right] \tag{10}$$

and

$$[1-Z^P_{N,S}(\omega)]=\int_0^{\infty}d\omega'\,\mathrm{Re}\left[\frac{\omega'}{[(\omega')^2-\Delta^2_{N,S}(\omega')]^{1/2}}\right]\int d\nu[\alpha^2_{N,S}F(\nu)+P_{N,S}(\nu)]\left[\frac{1}{\omega'+\omega+\nu-i0^+}-\frac{1}{\omega'-\omega+\nu-i0^+}\right], \tag{11}$$

where $\Delta_N(\omega)$ [$\Delta_S(\omega)$] is the complex gap as a function of real frequency for the normal N (superconducting S) side and $Z_N(\omega)$ [$Z_S(\omega)$] the renormalization functions. The first term on the right-hand side of (8) and (9) introduces into the equations the normal (N) superconducting (S) side phonons or paramagnons while the second term deals with the coupling between the two sides of the sandwich.

Solutions of the above equations for the gap are given in Fig. 3(a), where we show the real and imaginary part of $\Delta(\omega)$ on both normal and superconducting side. They apply to a Pb-normal metal junction with $\alpha^2_N F(\omega)$ taken to be zero and $P_N(\omega)$ a cutoff Lorentzian centered at 2.5 meV with width of 0.5 meV and a $\lambda_{SF}=0.5$ where

$$\lambda_{SF}=2\int\frac{P(\omega)}{\omega}d\omega$$

is the paramagnon electron mass renormalization parameter. These parameters were chosen for convenience but would not be completely unrealistic for the case of $TiBe_2$. We note that the imaginary part of each Δ_N and Δ_S start to be nonzero at a frequency equal to the normal side gap ($\Delta_N\cong 0.9$ meV). Also note that the real part of Δ_S has a small structure at this same frequency. The Pb transverse and longitudinal phonons are clearly seen in the real part of $\Delta_S(\omega)$ at approximately 5 and 10 meV, respectively, and, because the phonon spectral density $\alpha^2_S F(\omega)$ is attractive, the gap is increased at these frequencies. In contrast the real part of the normal side gap $\Delta_N(\omega)$ shows a large reduction at 3.5 meV reflecting the paramagnon spectral density $P_N(\omega)$ which is pair breaking and peaked around 2.5 meV. We stress that the paramagnon "hole" in Δ_N is displaced by the gap value $\Omega_N\cong 0.9$ meV so that it is centered around 3.5 meV. This very large feature due to the paramagnons will be reflected in the current-voltage (I-V) characteristics for tunneling on the normal side of the sandwich.

Before discussing I-V characteristic we discuss the explicit effect of paramagnons on the gap edge on the normal side of the junction. The BCS McMillan tunneling model for a system with $\Gamma_S=0$ and where no phonon or paramagnons are present in the normal side predicts an induced gap Ω_N that satisfies the equation

$$\frac{\Gamma_N}{\Omega_N}=\left[\frac{\Delta_S+\Omega_N}{\Delta_S-\Omega_N}\right]^{1/2}. \tag{12}$$

If this equation is used to estimate the induced gap edge of a system that actually has paramagnons, it would yield values much larger than the real ones. To understand this, let us go back to the Eliashberg equations (8)–(11) and approximate them using the two-square-well model for the electron-phonon interaction.[6,24]

We have that [Eqs. (8) and (9)]

$$\Delta_N(\omega)=\frac{\phi^P_N(\omega)+i\Gamma_N\Delta_S(\omega)/[\omega^2-\Delta^2_S(\omega)]^{1/2}}{Z^P_N(\omega)+i\Gamma_N/[\omega^2-\Delta^2_S(\omega)]^{1/2}}\ , \tag{13}$$

where ϕ^P_N and Z^P_N are given by Eqs. (10) and (11). We consider the case in which only paramagnons are present in the system, and neglect phonons and Coulomb repulsion. To obtain the gap edge we assume that $\Delta_N(\omega)$ is a constant equal to the induced gap edge Ω_N and that the paramagnon distribution $P_N(\Omega)$ can be approximated by a constant λ_{SF} for $\omega<\omega_{SF}$ and zero beyond. With these considerations:

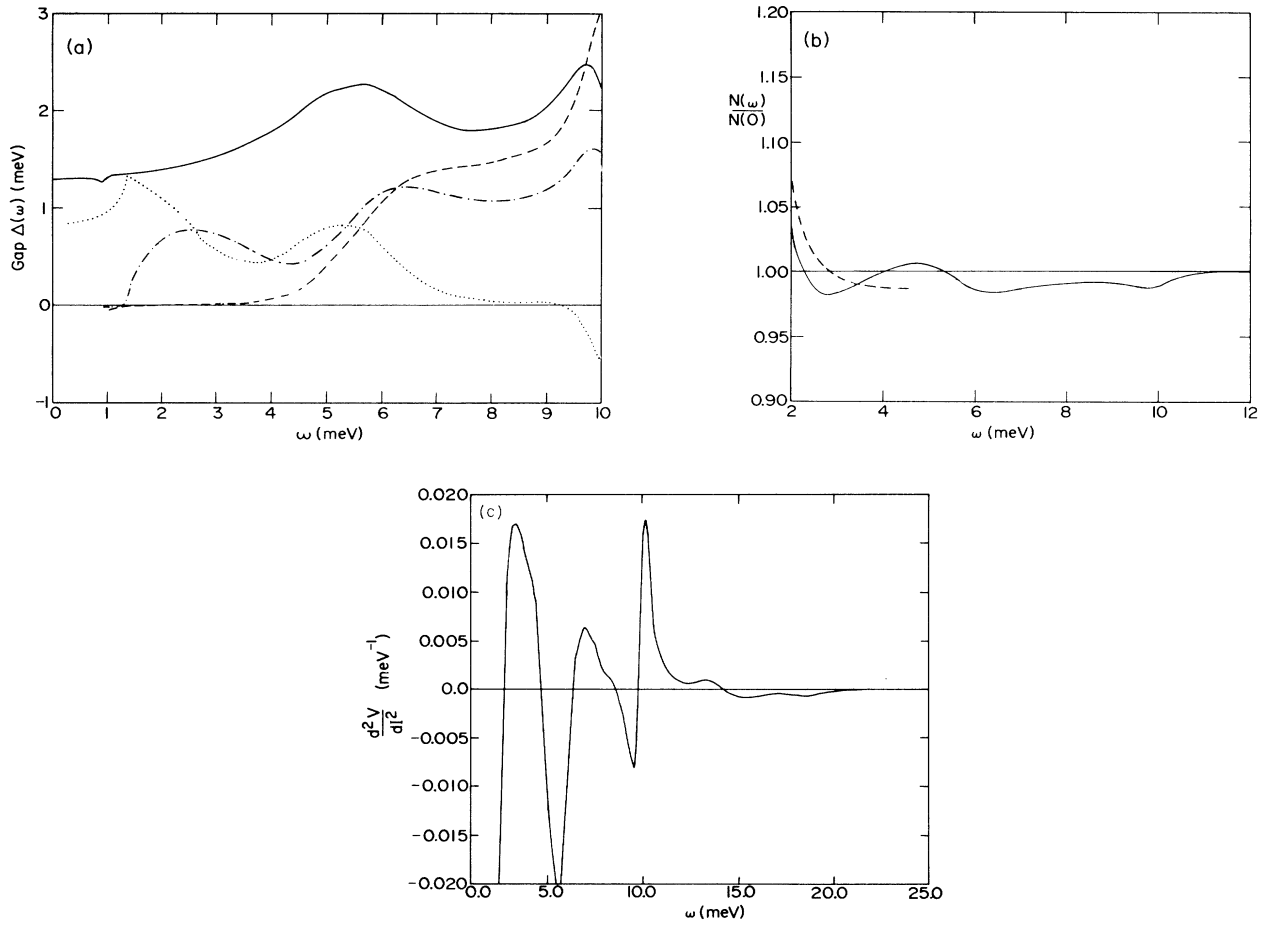

FIG. 3. Solution of the real axis Eliashberg equations for a material with a paramagnon distribution given by a Lorentzian at 2.5 meV with a width of 0.5 meV, $\lambda_{SF}=0.5$, and a Coulomb repulsion $\mu_N^*=0.1$ in proximity with Pb. The coupling constants are $\Gamma_N=6$ meV, $\Gamma_S=0.1$ meV. (a) gives the real and imaginary part of the gap function in the superconducting and normal side [——, $\mathrm{Re}\Delta_S(\omega)$; — — —, $\mathrm{Im}\Delta_S(\omega)$; · · · ·, $\mathrm{Re}\Delta_N(\omega)$; and —·—·—·, $\mathrm{Im}\Delta_N(\omega)$] in meV. (b) shows the tunneling density of states on the normal side of the junction in the paramagnon region (solid line), to be compared with the density of states of the normal side of the Pb-Cu (dashed line) proximity sandwich of approximately the same induced gap. (c) gives the second derivative of the I-V characteristics d^2V/dI^2 (in meV^{-1}) in the same frequency region.

$$\Omega_N=\frac{-\dfrac{\lambda_{SF}}{1+\lambda_{SF}}\displaystyle\int_{\Omega_N}^{\Omega_{SF}}\frac{\Omega_N}{(\omega^2-\Omega_N^2)^{1/2}}d\omega+\dfrac{\overline{\Gamma}_N\Delta_S}{(\Delta_S^2-\Omega_N^2)^{1/2}}}{1+\dfrac{\overline{\Gamma}_N}{(\Delta_S^2-\Omega_N^2)^{1/2}}}\,, \tag{14}$$

where

$$\overline{\Gamma}_N=\frac{\Gamma_N}{1+\lambda_{SF}}\,. \tag{15}$$

Solving the integral in this equation and assuming $\Omega_{SF}\gg\Omega_N$, we obtain after some simple algebra an approximated equation for the gap edge for a system where paramagnons are represented by a characteristic frequency Ω_{SF} and a renormalization constant λ_{SF}:

$$\left[1+\frac{\lambda_{SF}}{1+\lambda_{SF}}\ln\left[\frac{2\Omega_{SF}}{\Omega_N}\right]\right]\left[\frac{\Delta_S+\Omega_N}{\Delta_S-\Omega_N}\right]^{1/2}=\frac{\overline{\Gamma}_N}{\Omega_N}\,. \tag{16}$$

If $\lambda_{SF}=0$, Eq. (16) reduces to Eq. (12) if we use the renormalized $\overline{\Gamma}_N$ instead of Γ_N. The presence of the term with the logarithm reduces considerably the values of Ω_N that are solutions to (16) as compared with the solution to Eq. (12) for the same value of $\overline{\Gamma}_N$.

Table I gives the values of Ω_N obtained as solutions of Eqs. (12) and (16) to be compared with that obtained as a solution to the complete set of Eliashberg equations [Eqs. (8) and (11)] for several values of Γ_N. In all cases the paramagnon spectral density $P_N(\Omega)$ used in the complete equations [Eqs. (8) and (11)] was a Lorentzian peaking at 2.5 meV with a width of 2 meV. The first column of Table I gives Ω_N^{Re} as calculated from Eq. (12) with the renormalized $\overline{\Gamma}_N$ replacing Γ_N. Column 2 gives the $\Omega_N^{\mathrm{Eliash}}$

TABLE I. The zero-temperature gap edge on the normal side of the junction calculated from Eq. (12) with no paramagnons included (Ω_N^{Re}) compared with that from Eq. (16) with paramagnons (Ω_N^{BCS}). We see the drastic difference between these two results. Also given for comparison is $\Omega_N^{\mathrm{Eliash}}$, the gap edge obtained from full numerical solutions of Eqs. (8)—(11), which is seen to agree reasonably well with Ω_N^{BCS}.

Ω_N^{Re}	$\Omega_N^{\mathrm{Eliash}}$	Ω_N^{BCS}	Γ_N (meV)	λ_{SF}
0.24	0.10	0.10	0.5	0.7
0.46	0.25	0.26	1.0	0.5
1.02	0.78	0.81	5	0.7
1.28	0.94	0.95	6	0.5

as obtained with Eqs. (8)—(11) with the paramagnon distribution described above and a Coulomb repulsion $\mu^*=0.1$. The third column gives Ω_N^{BCS} obtained from Eq. (16) with $\Omega_{\mathrm{SF}}=3.0$ meV. We see that Eq. (16) agrees surprisingly well with the results of the full numerical calculations but that Eq. (12) in which paramagnons are ignored overestimates the gap edge on the normal site quite drastically. This is similar to the results obtained for the critical temperature in the preceding section and shows that paramagnons can have a drastic effect on superconducting properties. We will see this to be the case in the I-V characteristics which we now turn to.

The conductance $\sigma(V)$ at zero temperature is proportional to the quasiparticle density of states:

$$\sigma(V)=\frac{(dI/dV)_S}{(dI/dV)_N}=\mathrm{Re}\left[\frac{\omega}{[\omega^2-\Delta_N^2(\omega)]^{1/2}}\right]. \tag{17}$$

It is shown in Fig. 3(b). The important feature of this curve is the very marked dip centered around $V\equiv\omega=3$ meV which is due to the paramagnon spectral density of the normal metal. For comparison, and to emphasize this feature, the partial dashed curve shown is for the case of a proximity sandwich Pb-Cu with the same gap. The copper of course has no paramagnons. The contrast is striking and we conclude that paramagnons at low frequencies show up clearly in $\sigma(V)$ for the parameters chosen. In Fig. 3(c) we show the second derivative d^2V/dI^2 versus V for the same case as in the two previous figures. We emphasize the positive peak center roughly at 3.5 meV and extending from about 2.7 meV to 4.5 meV, which is a reflection of the corresponding dip in Fig. 3(a). This is due to the paramagnons. To end we note that for the curves just shown $\Gamma_N=6$ and Γ_S is very small. This value of Γ_N may be too large in realistic cases since in dealing with the transition metal Pd Dumoulin *et al.*[29] have found smaller values of the transmission coefficient and hence of Γ_N. We have made other calculations with smaller values of Γ_N but do not show these here since no new physics was found to emerge.

So far, we have considered only the case of Ω_{SF} sufficiently small that its characteristic structure will not interfere significantly with phonon structure and we have left $\alpha_N^2F(\omega)$ out of the calculations. This simulates the expected situation in $TiBe_2$. We wish now to consider the case when paramagnon and phonon characteristic energies are comparable in size. This may well be the case for Pd.[6]

In Fig. 4 we show the electron-phonon spectral density for Pd taken from a graph in the paper of Pinski *et al.*[30] These authors calculated this quantity from first principle and found that the mass enhancement (λ_N)

$$\lambda_N=\int 2\frac{\alpha_N^2F(\omega)}{\omega}d\omega \tag{18}$$

is 0.41 in Pd.[31] While it is not possible to know precisely the errors involved in these calculations, such a large value of λ_N would imply that pure Pd is superconducting unless paramagnons are present. We will not address the difficult question of the existence of paramagnons in Pd at this point but simply use the spectral density of Fig. 4 with several possible values of λ_N [readjusting accordingly the overall size of $\alpha_N^2F(\omega)$]. For the paramagnon spectral density $P_N(\omega)$ we make two choices so as to illustrate how they interfere with phonon structure if both characteristic energies should be roughly the same. The two models are triangular and shown in Fig. 4. In the first, which we will refer to as "with cancellation," the triangle is chosen so as to get cancellation of the peaks in $\alpha_N^2F(\omega)$, while in the second referred to as "with no cancellation" no special effort is made to produce maximum cancellation. Of course some cancellation does take place even in this case. Results for d^2V/dI^2 are found in Fig. 5. For these runs $\Gamma_N=1$ meV, $\Gamma_S\cong 0$, $\lambda_N=0.41$, and $\lambda_{\mathrm{SF}}=0.32$ with a normal side gap of $\Omega_N\cong 0.38$ meV. The top figure is for the model with no cancellation and considerable structure is seen in the phonon and paramagnon region. The phonon spectral density $\alpha^2F(\omega)$ has a peak at 17 meV, the peak in $P(\omega)$ is at 22 meV, and the longitudinal phonons are centered at 25 meV so that the relevant structure extends throughout the region 16 to 29 meV. Comparing this case with the one where $P(\omega)$ is chosen to cancel more effec-

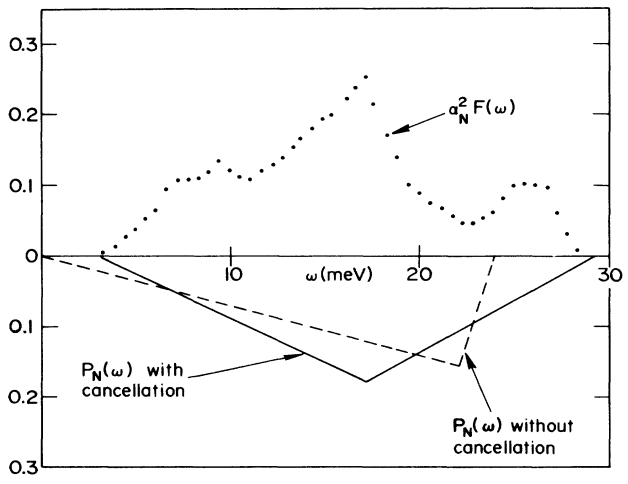

FIG. 4. The dotted line shows $\alpha^2F(\omega)$ for Pd from Ref. 30 with $\lambda_N=0.41$. The solid line gives one of the models chosen for $P_N(\omega)$ with $\lambda_{\mathrm{SF}}=0.32$. We refer to it in the text as "the one with cancellation." The dashed line gives the model for $P_N(\omega)$ "with no cancellation" and with the same value of λ_{SF}.

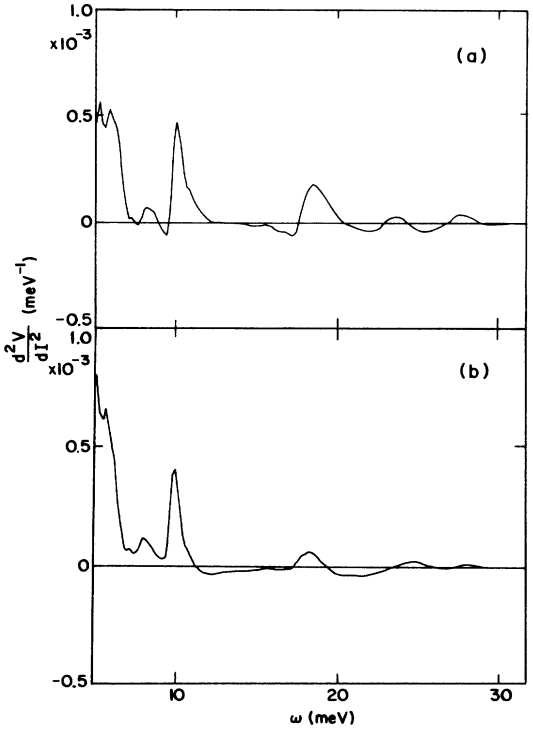

FIG. 5. d^2V/dI^2 (in meV^{-1}) for the normal side of a sandwich that has on the normal side the phonon and paramagnon distributions of Fig. 4. The top corresponds to the no cancellation model for $P(\Omega)$ and the bottom to the cancellation model $\lambda_N=0.41$ and $\lambda_{SF}=0.32$. A case with $\Gamma_N=1$ meV was chosen with a resulting induced gap of 0.35 meV in both cases.

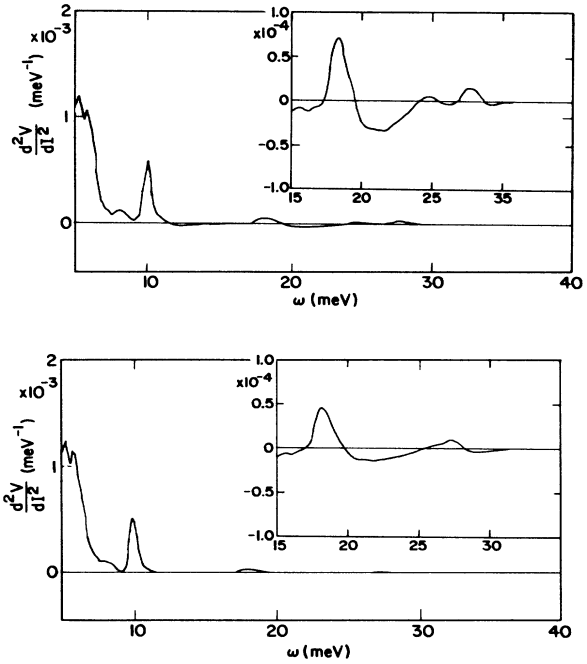

FIG. 6. $(d^2V/dI^2)|_{\text{normal}}$ (in meV^{-1}) for two systems where $\lambda_N-\lambda_{SF}=0.1$. The electron-phonon spectral density is the one of Fig. 4 but with a rescaling factor and $P(\Omega)$ is the cancellation model times a constant. The top figure is for a case with $\lambda_N=0.25$ and $\lambda_{SF}=0.15$ and an induced gap $\Omega_N=0.45$ meV ($\Gamma_N=0.97$ meV); the bottom one for $\lambda_N=0.1$ and $\lambda_{SF}=0$ with the same induced gap ($\Gamma_N=0.77$ meV).

tively against $\alpha_N^2F(\omega)$ (lower curve) we see a very large reduction of the Pd structure in this second instance. We can conclude from this figure that, as anticipated by Mitrović,[6] the Pd phonon structure can be reduced by the presence of paramagnons if $P_N(\omega)$ largely cancels against $\alpha^2F_N(\omega)$ as a function of frequency. For the cancellation to be effective, however, it must be a local frequency by frequency cancellation and so both distributions need to be of similar shape. For example, while we have chosen a triangular distribution for $P_N(\omega)$ when its peak is taken to fall near 17 meV, its shape is not so different from $\alpha^2F(\omega)$ in Pd.

To illustrate these effects further we have considered a somewhat different case in Fig. 6. What is shown in Fig. 6(a) are results for a case with $\Gamma_N=0.97$ meV, $\Gamma_S\cong 0$, $\Omega_N=0.43$ meV, and $\lambda_N=0.25$ with $\lambda_{SF}=0.15$ so that the difference $\lambda_N-\lambda_{SF}=0.1$. This is to be compared with the case $\Gamma_N=0.77$, $\Omega_N=0.42$ meV (the same gap) but with no spin fluctuation and λ_N itself taken to be 0.1 [Fig. 6(b)]. In both figures $\mu^*=0.1$ so that, in effect, the Pd has no net attraction: $\lambda_N-\lambda_{SF}-\mu^*=0$ in both instances. What is important to realize is that even though we have chosen $P(\omega)$ to cancel substantially against $\alpha_N^2F(\omega)$ the Pd structure that we get in the first model $\lambda_N=0.25$, $\lambda_{SF}=0.15$ is much larger than for no paramagnons and $\lambda_N=0.1$. Thus the cancellation is not complete as expected from Fig. 4. It would, however, be quite artificial to try to have even more cancellation since then we would need to have $P_N(\omega)$ reflect tightly the shape of the electron-phonon distribution, something which is not expected.

Before we turn to a more specific discussion of the case of Pd for which tunneling results exist (Dumoulin *et al.*[29]) we make one more point which is essential for understanding the d^2V/dI^2 structure in this case. Referring to Fig. 6 it is important to realize that for the case $\lambda_N=0.1$ and no paramagnons, the amount of phonon structure obtained is considerably less than would have been the case for a Al shape spectrum. Al exhibits a large sharp longitudinal peak which would lead to a large structure in d^2V/dI^2 even if the spectral weight is reduced to $\lambda_N=0.1$. Because the phonon structure in the Pd spectrum of Fig. 4 is more evenly spread among several frequencies with a main peak at 17 meV and only a small longitudinal peak beyond, it does not produce as sharp a structure. A consequence of this is that the phenomenological technique developed to extract a value of λ_N from d^2V/dI^2 structure would substantially underestimate it. This was discussed in some detail within the context of Cu-Pb proximity sandwich by Zarate and Carbotte[23] to which we refer the reader.

IV. THE SPECIFIC CASE OF Pd

The aim of this section is to analyze in some detail the specific case of Pd and to see what normal-state parame-

ters are most consistent with the present experimental knowledge of its properties. In making this assessment we will want to consider besides the theoretical estimate of $\lambda_N=0.4$ in Pd, the possibility of some paramagnons as well as the tunneling results of Dumoulin *et al.*[29] In addition, the important de Haas–Van Alphen work of Dye *et al.*[32] needs to be included. These authors conclude that the sum of $\lambda_N+\lambda_{SF}\cong 0.4$ in Pd. Finally, we should not violate the observation that pure Pd does not superconduct and also that irradiated Pd, which has a reduced spin susceptibility,[33] has a T_c of 3 K.[34] All these data are to be kept in mind in what follows.

First, let us go back to Fig. 6. The Pd structure found in this figure is smaller than that observed in the experiment of Dumoulin *et al.*,[29] indicating that $\lambda_N=0.1$, $\lambda_{SF}=0.0$ or $\lambda_N=0.25$, $\lambda_{SF}=0.15$ with $\mu^*=0.1$ is not consistent with experiment and a value of the effective $\lambda_N-\lambda_{SF}$ larger than 0.1 is needed. After a considerable amount of trial and error we arrived at the model shown in Fig. 7(a). It has $\lambda_N=0.275$, $\lambda_{SF}=0.125$, and $\mu^*=0.15$ with a gap $\Omega_N=0.59$ meV. The amount of Pd structure seen is now in agreement with experiment. Also, $\lambda_N+\lambda_{SF}=0.4$ is in agreement with the de Haas–van Alfen data. The net interaction in Pd measured by $\lambda_N-\lambda_{SF}-\mu^*=0$ is consistent with no superconductivity for pure Pd. Further, $\lambda_N=0.275$ is not so far off the theoretical value of 0.41 considering the considerable uncertainties in such calculated values. Finally, if we assume that λ_N of irradiated Pd is about the same as in pure Pd, but that the spin fluctuations have been suppressed, a net interaction of $\lambda_N-\mu^*=0.125$ is not inconsistent with a critical temperature of 3 K.

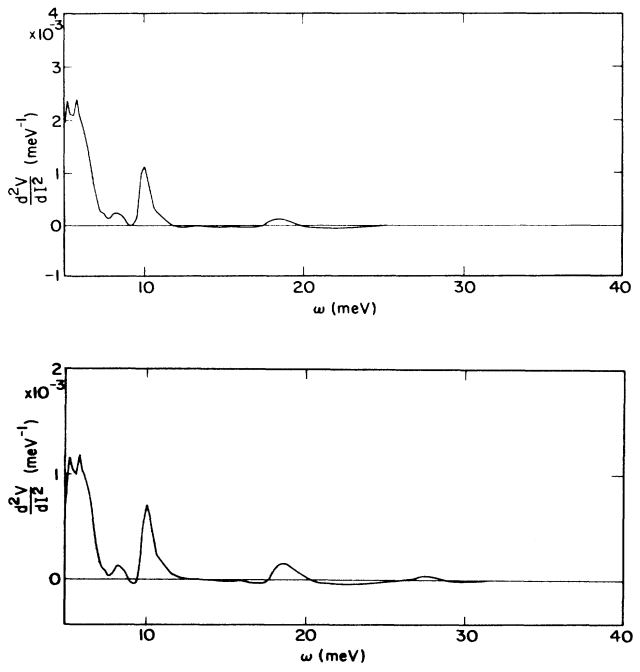

FIG. 7. $(d^2V/dI^2)|_{\text{normal}}$ (in meV^{-1}) for $\alpha^2(\omega)F(\omega)$ of Pd (Fig. 4) (a) with $\lambda_N=0.275$, $P(\omega)$ given by the cancellation model of Fig. 4 with $\lambda_{SF}=0.125$, and $\mu^*=0.15$. The induced gap is 0.63 meV ($\Gamma_N=1.6$ meV). (b) has $\lambda_N=0.3$, $\lambda_{SF}=0.1$, and a gap $\Omega_N=0.55$ meV ($\Gamma_N=1.2$ meV). It is included for comparison and shows structure in the phonon-paramagnon region which is larger than found experimentally.

The final model shown, for comparison in Fig. 7(b), is for $\lambda_N=0.3$, $\lambda_{SF}=0.1$, and a gap $\Omega_N=0.52$ meV. In this case $\lambda_N-\lambda_{SF}=0.2$, which is larger than the value of 0.15 considered in the previous example. The overall Pd structure is now a little too large to agree with experiment indicating that $\lambda_N-\lambda_{SF}$ cannot be very different from 0.15 if we are to get agreement with tunneling unless of course, by accident, there was a more complete cancellation of $\alpha^2F_N(\omega)$ against $P_N(\omega)$ than contemplated here. Finally, if no paramagnons are included within the phonon region the tunneling structure requires that $\lambda_N<0.2$. This would lead to a violation of the de Haas–van Alphen data, increase seriously the discrepancy with the calculated theoretical value of λ_N, and would provide no explanation of the irradiated Pd results.

V. CONCLUSIONS

We have studied several aspects of the superconducting properties of a proximity sandwich in which paramagnons of low energies are assumed to exit on the normal side. Our analysis of the critical temperature of the junction T_c^{NS} indicates that it is strongly affected by the paramagnons and that for a paramagnon mass renormalization parameter $\lambda_{SF}=0.7$, its value drops towards zero with increasing barrier parameter Γ_s much more rapidly than in the corresponding case of zero net interaction on the normal side. The pattern of behavior obtained cannot be entirely simulated by a redefinition of the unknown McMillan proximity parameter Γ_N. Further, from consideration of the functional derivative of T_c^{NS} with paramagnon spectral density $P_N(\omega)$ it is concluded that paramagnons are increasingly more effective in depressing T_c^{NS} as their frequency Ω_{SF} is lowered. This behavior is in contrast to the case of phonons for which an optimum frequency exists around $7k_BT_c^{NS}$ for enhancement of the critical temperature.

Consideration of the normal side gap edge Ω_N in a simple model (which is found to be qualitatively correct) indicates that Ω_N is also very much affected by the presence of paramagnons on the normal side and that data on Ω_N cannot be interpreted without explicit inclusion of paramagnons.

Solutions of a set of four coupled Eliashberg equations are generated on the real axis for several cases, but mainly two models are considered. The first, which may be fairly realistic in the case of $TiBe_2$, takes the electron paramagnon mass renormalization parameter $\lambda_{SF}=0.5$ and the characteristic energy $\Omega_{SF}=2.5$ meV. In the second model $\lambda_{SF}\cong 0.1$ and $\Omega_{SF}\cong 25$ meV, parameters that are sometime quoted for Pd. In addition, some variations of these parameters are considered when this is found useful.

From accurate solutions of the real axis Eliashberg equations, tunneling characteristics are calculated for the normal side of the sandwich. Large characteristic structures were found in the second derivative of voltage (V) with current (I) reflecting the paramagnon spectral densi-

ty for $\lambda_{SF}=0.5$ and $\omega_{SF}=2.5$ meV and from which information can be derived on the shape and strength of the spectral function. Because of the low paramagnon energy characteristic of $TiBe_2$, no phonons were considered on the normal side of the sandwich in the above calculations since they would not overlap. Next we studied the interplay of phonons with paramagnons where they possess similar characteristic energies, as is likely to be the case in Pd. It was found that some cancellation of paramagnon and phonon structure in d^2V/dI^2 can occur when the spectra have very similar shapes. This was first emphasized by Mitrović. Complete cancellation, however, requires a frequency by frequency matching of the two distributions.

Turning more specifically to the recent data of Dumoulin *et al.*[29] on Pd, several calculations were done to try to understand these data. We find that a very important idea in the interpretation of the data is the realization that the calculated electron-phonon spectral density of Pinski *et al.*[30,31] for Pd does not show a large distinct peak at the longitudinal phonon energy. Instead, its prominent peak is around 17 meV. This implies that the usual phenomenological prescription for deducing λ_N from the high-energy peak would importantly underestimate its value while the 17-meV peak cannot be used because it is far from Lorentzian in shape. These effects were discussed in detail by Zarate and Carbotte for Cu-Pb junctions. The reader is referred to their paper for more explanation.

In addition to the phonons, if paramagnons exist in Pd in a significant amount they could reduce the phonon structure. In fact a triangular shape for $P(\omega)$ with a peak around the Debye energy which may not be unrealistic for Pd does lead to significant cancellation. With such a model we are able to get reasonable agreement with the amount of structure observed in tunneling assuming $\lambda_N=0.275$, $\lambda_{SF}=0.125$, and $\mu^*=0.15$. This implies that there would be no net attraction in Pd as measured by $\lambda_N-\lambda_{SF}-\mu^*=0$. This model is consistent with (a) no superconductivity in pure palladium, (b) the de Haas–van Alphen data indicating $\lambda_N+\lambda_{SF}\cong 0.4$, (c) the theoretical estimate that $\lambda_N\cong 0.4$, and (d) the observation of $T_c\cong 3$ K for irradiated Pd, assuming that the major change brought about by irradiation is the suppression of the paramagnons. If instead of the above we chose $\lambda_N=0.3$ and $\lambda_{SF}=0.1$, so that $\lambda_N-\lambda_{SF}\cong 0.2$ rather than 0.15, the predicted tunneling structure from Pd would be too large while $\lambda_N=0.25$ and $\lambda_{SF}=0.15$ give too little. This indicates that $\lambda_N-\lambda_{SF}$ in Pd cannot be very different from 0.15 unless of course more cancellation occurs between α_N^2F and $P_N(\omega)$ than anticipated here, something which is possible but unlikely.

ACKNOWLEDGMENTS

This research was supported in part by the Natural Sciences and Engineering Research Council (NSERC) of Canada. We thank E. Schachinger for help.

APPENDIX: FUNCTIONAL DERIVATIVE $\delta T_c^{NS}/\delta P(\omega)$

In this appendix we derive a simple, approximate, but analytic expression for the functional derivative of the sandwich critical temperature with respect to the normal state paramagnon spectral density. In Eqs. (3) and (4) for the normal side pairing energy and renormalization we add to $P(\omega)$ a delta function contribution at $\omega=\Omega_0$ with infinitesimal weight ϵ. We treat this addition exactly but use, for the remaining part $\lambda_N^-(m,n)$, the approximation that it is a constant for $|\omega_n|$, $|\omega_m|$ both less than some cutoff frequency (ω_D) and zero otherwise. If further, for simplicity, we take $\lambda_N^- -\mu_N^*=0$, i.e., no net interaction on the normal side, we get

$$\tilde{\Delta}_N(n)=\Gamma_N\frac{\tilde{\Delta}_S(n)}{|\tilde{\omega}_S(n)|}+\epsilon\pi T_c\sum_m\frac{-2\Omega_0}{\Omega_0^2+(\omega_n-\omega_m)^2}\frac{\tilde{\Delta}_N(m)}{|\tilde{\omega}_N(m)|} \tag{A1}$$

with

$$|\tilde{\omega}_N(n)|=|\omega_n|(1+\lambda_N^+)+\Gamma_N+\epsilon f_N \equiv|\tilde{\omega}_N^0(n)|+\epsilon f_n\ . \tag{A2}$$

Here

$$f_n=\pi T_c\sum_m\frac{2\Omega_0\mathrm{sgn}(\omega_n\omega_m)}{\Omega_0^2+(\omega_n-\omega_m)^2}\ . \tag{A3}$$

Using the same kind of approximation for the superconducting side, we obtain

$$\tilde{\Delta}_S(n)=\tilde{\Delta}_S^0+\Gamma_S\frac{\tilde{\Delta}_N(n)}{|\tilde{\omega}_N(n)|} \tag{A4}$$

with (no paramagnons on the S side)

$$\tilde{\Delta}_S^0=(\lambda_S-\mu_S^*)\pi T_c\sum_m\frac{\tilde{\Delta}_S(m)}{|\tilde{\omega}_S(m)|} \tag{A5}$$

and

$$|\tilde{\omega}_S(n)|\equiv|\tilde{\omega}_S^0(n)|=|\omega_n|(1+\lambda_S)+\Gamma_S\ . \tag{A6}$$

In Eq. (A1), $\tilde{\Delta}_N(m)/|\tilde{\omega}_N(m)|$ can be replaced by $\Gamma_N\tilde{\Delta}_S(m)/|\tilde{\omega}_S(m)|$ to lowest order in ϵ and substitution of this into (A4) for $\tilde{\Delta}_S(n)$ gives after some rearrangement

$$\tilde{\Delta}(n)=\frac{|\tilde{\omega}_N(n)|\,|\tilde{\omega}_S(n)|}{|\tilde{\omega}_N(n)|\,|\tilde{\omega}_S(n)|-\Gamma_S\Gamma_N}\left[\tilde{\Delta}_S^0+\epsilon\frac{\Gamma_N\Gamma_S}{|\tilde{\omega}_N(n)|}\pi T_c\sum_m\frac{-2\Omega_0\tilde{\Delta}_S(m)}{\Omega_0^2+(\omega_n-\omega_n)^2}\frac{1}{|\tilde{\omega}_N(m)|\,|\tilde{\omega}_S(m)|}\right]. \tag{A7}$$

Noting that in the last term on the right-hand side of (A7) we can replace $\tilde{\Delta}_S^0(m)$ by $\tilde{\Delta}_S^0$ to lowest order in ϵ and then substitution into (A5), yields the eigenvalue equation

$$1=(\lambda_S-\mu_S^*)\pi T_c\sum_n \frac{|\tilde{\omega}_N(n)|}{|\tilde{\omega}_N(n)|\ |\tilde{\omega}_S(n)|-\Gamma_S\Gamma_N}\left[1+\epsilon\frac{\Gamma_N\Gamma_S}{|\tilde{\omega}_N(n)|}\pi T_c\sum_m \frac{-2\Omega_0}{\Omega_0^2+(\omega_n-\omega_m)^2}\frac{1}{|\tilde{\omega}_N(m)|\ |\tilde{\omega}_S(m)|}\right]. \quad \text{(A8)}$$

Substitution of (A3) into this last equation and working to first order in ϵf_n yields after some algebra

$$1=(\lambda_S-\mu_S^*)\pi T_c\sum_n \frac{|\tilde{\omega}_N^0(n)|}{|\tilde{\omega}_N^0(n)|\ |\tilde{\omega}_S^0(n)|-\Gamma_S\Gamma_N}+\epsilon\Gamma_N\Gamma_S(\lambda_S-\mu_S^*)A(\Omega_0) \quad \text{(A9)}$$

with

$$A(\Omega_0)=(\pi T_c)^2\sum_{n,m}\left[\frac{1}{|\tilde{\omega}_S^0(n)|\ |\tilde{\omega}_N^0(n)|-\Gamma_S\Gamma_N}\left[-\frac{2\Omega_0}{\Omega_0^2+(\omega_n-\omega_m)^2}\right]\frac{1}{|\tilde{\omega}_N^0(m)|\ |\tilde{\omega}_S^0(m)|-\Gamma_S\Gamma_N}\right.$$
$$\left.-\frac{1}{[|\tilde{\omega}_S^0(n)|\ |\tilde{\omega}_N^0(n)|-\Gamma_S\Gamma_N]^2}\frac{2\Omega_0\mathrm{sgn}(\omega_n\omega_m)}{\Omega_0^2+(\omega_n-\omega_m)^2}\right]. \quad \text{(A10)}$$

Ignoring the ϵ correction in (A9) yields the critical temperature of the sandwich T_c^0 before augmentation of the paramagnon spectral density which is given some simple algebra by the equation

$$1=\left[\frac{\lambda_S-\mu_S^*}{1+\lambda_S}\right]\left\{\ln\left[\frac{1.13\omega_D}{k_BT_c^0}\right]+\frac{\bar{\Gamma}_S}{\bar{\Gamma}}\left[\psi\left[\frac{\bar{\Gamma}}{2\pi k_BT_c^0}+\frac{1}{2}\right]-\psi(\tfrac{1}{2})\right]\right\}, \quad \text{(A11)}$$

where ψ is a digamma function $\bar{\Gamma}\equiv\bar{\Gamma}_S+\bar{\Gamma}_N$ and $\bar{\Gamma}_S=\Gamma_S/(1+\lambda_S^+)$, $\bar{\Gamma}_N=\Gamma_N/(1+\lambda_N^+)$. When ϵ is left in Eq. (A9) the first term on the right-hand side also takes on the form (A11) but now with $T_c=T_c^0+\delta T_c$, which means that we get

$$\ln\left[\frac{T_c}{T_c^0}\right]=-\frac{\bar{\Gamma}_S}{\bar{\Gamma}}\left[\psi\left[\frac{\bar{\Gamma}}{2\pi k_BT_c}+\frac{1}{2}\right]-\psi\left[\frac{\bar{\Gamma}}{2\pi k_BT_c^0}+\frac{1}{2}\right]\right]+\epsilon A(\Omega_0)\Gamma_N\Gamma_S(1+\lambda_S). \quad \text{(A12)}$$

Expanding T_c in terms of T_c^0 and δT_c in (A12) yields

$$\delta T_c=\frac{T_c^0\epsilon A(\Omega_0)\Gamma_N\Gamma_S(1+\lambda_S)}{1-(\bar{\Gamma}_S/2\pi k_BT_c^0)\psi'(\bar{\Gamma}/2\pi k_BT_c^0+\frac{1}{2})} \quad \text{(A13)}$$

so that ($\bar{\Omega}_0=\Omega_0/\pi T_c^0$)

$$\frac{\delta T_c}{\delta P(\Omega_0)}=\frac{\bar{\Gamma}_N\bar{\Gamma}_S}{\pi(1+\lambda_N^+)}\frac{1}{1-(\bar{\Gamma}_S/2\pi k_BT_c^0)\psi'(\bar{\Gamma}/2\pi k_BT_c^0+\frac{1}{2})}$$
$$\times\sum_{m,n}\frac{2\bar{\Omega}_0}{\bar{\Omega}_0^2+(2n-2m)^2}\frac{1}{\pi^2(T_c^0)^2}\times\left[\frac{1}{|2n-1|(|2n-1|+\bar{\Gamma}/\pi T_c^0)}\right]$$
$$\times\left[-\frac{1}{|2m-1|(|2m-1|+\bar{\Gamma}/\pi T_c^0)}-\frac{\mathrm{sgn}[(2m-1)(2n-1)]}{|2n-1|(|2n-1|+\bar{\Gamma}/\pi T_c^0)}\right]. \quad \text{(A14)}$$

The sums in (A14) can be done numerically for a given value of $\bar{\Omega}_0$ and $\bar{\Gamma}/\pi T_c^0$ with $T_c^0\equiv T_c^{\mathrm{NS}}$—the sandwich critical temperature.

[1]G. Gladstone, M. A. Jensen, and J. R. Schrieffer, in *Superconductivity,* edited by R. D. Parks (Marcel Dekker, New York, 1969), Vol. 2, p. 665.

[2]R. A. Webb, J. B. Ketterson, W. P. Halperin, J. J. Vuillemin, and N. B. Sandesara, J. Low Temp. Phys. **32**, 659 (1978).

[3]P. F. de Chatel and E. P. Wohlfarth, Comments Solid State Phys. **5**, 133 (1973).

[4]M. T. Beal-Monod, Physica **109&110B**, 1837 (1982).

[5]F. J. Pinski, P. B. Allen, and W. H. Butler, Phys. Rev. B **23**, 5086 (1981).

[6]B. Mitrović, Solid State Commun. **47**, 51 (1983).

[7]W. Gerhardt, F. Razavi, J. R. Schilling, D. Hüser, and J. A. Mydosh, Phys. Rev. B **24**, 6744 (1981).

[8]W. Gerhardt, J. S. Schilling, H. Olijnyk, and J. L. Smith, Phys. Rev. B **28**, 5814 (1983).

[9]G. R. Stewart, J. L. Smith, A. L. Giorgi, and Z. Fisk, Phys. Rev. B **25**, 5907 (1982).

[10]G. R. Stewart, J. L. Smith, and B. L. Brandt, Phys. Rev. B **26**, 3783 (1982).

[11]S. Doniach and S. Engelsberg, Phys. Rev. Lett. **17**, 750 (1966).

[12]N. F. Berk and J. R. Schrieffer, Phys. Rev. Lett. **17**, 433 (1966).

[13]P. Hertel, J. Appel, and D. Fay, Phys. Rev. B **22**, 534 (1980).
[14]H. Rietschel and H. Winter, Phys. Rev. Lett. **43**, 1256 (1979); Phys. Rev. B **22**, 4284 (1980).
[15]H. Rietschel, Phys. Rev. B **24**, 155 (1981).
[16]R. Baquero, J. M. Daams, and J. P. Carbotte, J. Low Temp. Phys. **42**, 585 (1981).
[17]J. M. Daams, B. Mitrović, and J. P. Carbotte, Phys. Rev. Lett. **46**, 65 (1981).
[18]B. Mitrović and J. P. Carbotte, Solid State Commun. **41**, 695 (1982).
[19]J. Zasadzinski, D. M. Burnell, E. J. Wolf, and G. B. Arnold, Phys. Rev. B **25**, 1622 (1982).
[20]C. R. Leavens and A. H. MacDonald, Phys. Rev. **27**, 2812 (1983).
[21]J. M. Daams, J. P. Carbotte, M. Ashraf, and R. Baquero, J. Low Temp. Phys. **55**, 1 (1984).
[22]W. L. McMillan, Phys. Rev. **175**, 537 (1968); **175**, 559 (1968).
[23]H. G. Zarate and J. P. Carbotte, J. Low Temp. Phys. **59**, 19 (1985).
[24]P. Fulde and A. Luther, Phys. Rev. **170**, 570 (1968).
[25]W. F. Brinkman and S. Engelsberg, Phys. Rev. Lett. **21**, 1187 (1968).
[26]J. Appel, D. Fay, and P. Hertel, Phys. Rev. B **31**, 2754 (1985).
[27]M. T. Béal-Monod, Physica **109&110B**, 1837 (1982).
[28]W. L. McMillan and J. M. Rowell, in *Superconductivity,* edited by R. D. Parks (Marcell Dekker, New York, 1969), Vol. 1, p. 561.
[29]L. Dumoulin, P. Nedellec, and P. M. Chaikin, Phys. Rev. Lett. **47**, 208 (1981).
[30]F. J. Pinski, P. B. Allen, and W. H. Butler, J. Phys. (Paris) Colloq. **39**, C6-472 (1978).
[31]F. J. Pinski, P. B. Allen, and W. H. Butler, Phys. Rev. Lett. **41**, 431 (1978).
[32]D. H. Dye, S. A. Campbell, G. W. Crabtree, J. B. Ketterson, N. B. Sandesara, and J. J. Vuillemin, Phys. Rev. **23**, 462 (1981).
[33]J. D. Meyer and B. Stritzler, Phys. Rev. Lett. **48**, 502 (1982).
[34]B. Stritzker, Phys. Rev. Lett. **42**, 1769 (1979).